Cells Tissues Organs

Engineered Vascular Tissue Fabricated from Aggregated Smooth Muscle Cells

Tracy A. Gwyther   Jason Z. Hu   Alexander G. Christakis   Jeremy K. Skorinko
Sharon M. Shaw   Kristen L. Billiar   Marsha W. Rolle

Department of Biomedical Engineering, Worcester Polytechnic Institute, Worcester, Mass., USA

Key Words

Biomechanics · Cell-derived matrix · Smooth muscle cell · Vascular tissue engineering

Abstract

The goal of this study was to develop a system to rapidly generate engineered tissue constructs from aggregated cells and cell-derived extracellular matrix (ECM) to enable evaluation of cell-derived tissue structure and function. Rat aortic smooth muscle cells seeded into annular agarose wells (2, 4 or 6 mm inside diameter) aggregated and formed thick tissue rings within 2 weeks of static culture (0.76 mm at 8 days; 0.94 mm at 14 days). Overall, cells appeared healthy and surrounded by ECM comprised of glycosoaminoglycans and collagen, although signs of necrosis were observed near the centers of the thickest rings. Tissue ring strength and stiffness values were superior to those reported for engineered tissue constructs cultured for comparable times. The strength (100–500 kPa) and modulus (0.5–2 MPa) of tissue rings increased with ring size and decreased with culture duration. Finally, tissue rings cultured for 7 days on silicone mandrels fused to form tubular constructs. Ring margins were visible after 7 days, but tubes were cohesive and mechanically stable, and histological examination confirmed fusion between ring subunits. This unique system provides a versatile new tool for optimization and functional assessment of cell-derived tissue, and a new approach to creating tissue-engineered vascular grafts.

Copyright © 2011 S. Karger AG, Basel

T.A.G. and J.Z.H. contributed equally to this work.

Introduction

Over the past three decades, tissue engineering has emerged as a promising approach to create blood vessel substitutes for clinical transplantation, as well as model systems to study vascular tissue function in vitro. To date, the majority of strategies for tissue-engineered blood vessel (TEBV) synthesis have involved seeding cells within scaffolds made from synthetic [Shinoka et al., 1998; Nik-

Abbreviations used in this paper	
DMEM	Dulbecco's modified Eagle's medium
ECM	extracellular matrix
FBS	fetal bovine serum
MTM	maximum tangent modulus
PDMS	polydimethyl siloxane
SMC	smooth muscle cell
TEBV	tissue-engineered blood vessel
UTS	ultimate tensile strength

Dr. Marsha W. Rolle
Department of Biomedical Engineering
Worcester Polytechnic Institute
100 Institute Road, Worcester, MA 01609 (USA)
Tel. +1 508 831 4145, Fax +1 508 831 4121, E-Mail mrolle@wpi.edu

lason et al., 1999; Opitz et al., 2004; Hashi et al., 2007; Nieponice et al., 2008] or natural polymers [Weinberg and Bell, 1986; Seliktar et al., 2000; Grassl et al., 2003; Swartz et al., 2005; Stegemann et al., 2007; Zavan et al., 2008]. Alternatively, 'scaffold-free' tissue engineering approaches have been explored in which TEBV are fabricated entirely from self-assembled cells and cell-derived extracellular matrix (ECM), such as rolling cultured cell sheets [L'Heureux et al., 1998; Gauvin et al., 2010], organ printing [Mironov et al., 2009; Norotte et al., 2009] or assembly and fusion of clustered cells [Kelm et al., 2010]. Autologous vascular grafts produced by the cell sheet-based engineering method exhibit comparable tensile strength to human saphenous veins [Konig et al., 2009] although graft fabrication and maturation requires 2–3 months [L'Heureux et al., 2006]. However, vascular grafts created with this method have already shown clinical promise as arteriovenous fistulas [McAllister et al., 2009].

Despite the promise and increasing number of reports using cell-based approaches to tissue engineering, few studies to date have examined the mechanical strength or other functional properties of engineered tissue constructs created entirely from cells and cell-derived ECM. Safe and successful in vivo application of TEBV made entirely from cells will depend on achieving adequate strength and mechanical stability. The aim of this study was therefore to develop a simple system to generate strong three-dimensional tissue constructs from aggregated cells within an experimentally useful time frame (1–2 weeks) in a format that is conducive to mechanical and physiological testing. To achieve this aim, we chose to create ring-shaped constructs due to their simple geometry and the precedent for using vascular tissue rings for mechanical and physiological analysis of blood vessel function. We predict that this model system will enable systematic assessment of the roles of cell source and culture parameters on cell-derived tissue structure and function.

To create ring-shaped tissue constructs, rat aortic smooth muscle cells (SMCs) were seeded into custom round-bottomed, annular wells cast in agarose, with post sizes of 2, 4 or 6 mm (to produce rings with 2, 4 or 6 mm inner diameters). Tissue rings were cultured for 8 or 14 days prior to thickness measurements and analysis of handling and mechanical properties. Uniaxial tensile testing was performed to measure ultimate tensile strength, stiffness and failure strain, and tissue structure and ECM composition were examined by histology. Finally, we assessed the feasibility of using tissue rings as subunits to generate larger, tube-shaped constructs.

Materials and Methods

Custom Cell Culture Well Fabrication

A custom polycarbonate mold was created by machining annular wells with inner post diameters of 2, 4 and 6 mm (Small Parts Inc., Miramar, Fla., USA). The wells were machined with round bottoms to facilitate cell settling and self-aggregation to form rings. Polydimethylsiloxane (PDMS, Sylgard 184; Dow Corning, Midland, Mich., USA) was mixed at a 10:1 ratio (w/w) of base to curing agent, degassed for 2 h, and poured onto the polycarbonate mold. After curing at 60°C for 4 h, the PDMS was peeled from the mold and used as a template. Two percent agarose (w/v; Lonza, Rockland, Me., USA) was dissolved in Dulbecco's modified Eagle medium (DMEM; Mediatech, Herndon, Va., USA), autoclaved and poured onto the PDMS template to form the wells for cell seeding. Individual agarose wells were cut away from the PDMS template and placed into 6-well plates. The agarose wells were incubated in DMEM supplemented with 10% fetal bovine serum (FBS; PAA, Etobicoke, Ont., Canada) and 1% penicillin/streptomycin (Mediatech) and equilibrated in an incubator for 1 h prior to cell seeding at 37°C and 5% CO_2. A schematic of this process is shown in figure 1.

SMC Culture and Seeding

Rat aortic SMCs (WKY 3M-22; a cell line derived from SMCs isolated from 3-month-old adult male Wistar-Kyoto rat aortas by enzymatic digestion [Lemire et al., 1994; Lemire et al., 1996]; generously provided by Dr. Thomas Wight) were cultured in DMEM (Mediatech) supplemented with 10% FBS (PAA) and 1% penicillin/streptomycin (Mediatech). At 90% confluence, SMCs were trypsinized and re-suspended in culture medium. The number of SMCs seeded into each well was scaled to the size of the channel (0.66, 1.3 and 2.0×10^6 cells per well seeded into 2-, 4- and 6-mm inner diameter wells, respectively). Plates were left undisturbed in the incubator for the first 48 h after seeding, after which the culture medium was changed every 48 h for the duration of the 8- or 14-day culture period. Four batches of 2-, 4- and 6-mm rings were produced for mechanical testing studies (two batches harvested at 8 days and 2 batches harvested at 14 days) as described below. An additional two batches (one at each time point) of 4-mm rings were created for histological evaluation of tissue rings not subjected to mechanical testing (3 rings per time point).

Tissue Ring Thickness Measurements

On the final day of each study, the tissue rings were removed from the agarose wells and transferred to 60-mm Petri dishes filled with phosphate-buffered saline (PBS) at room temperature. The rings were centered under a machine vision system (model 630; DVT Corporation, Atlanta, Ga., USA) and thickness measurements were acquired in three separate positions along the circumference of the ring using edge detection software (Framework 2.4.6; DVT). Three measurements were averaged to yield a mean thickness value for each sample.

Mechanical Testing

Mechanical properties of tissue rings were measured using a uniaxial testing machine (ElectroPuls E1000; Instron, Norwood, Mass., USA). The tissue rings were mounted between two small stainless steel pins (referred to as 'grips') and submerged in PBS. One grip was connected to an electromagnetic actuator and the

Gwyther/Hu/Christakis/Skorinko/Shaw/Billiar/Rolle

Fig. 1. Tissue ring production process. Schematic of tissue ring mold formation (**a**). PDMS was poured into a polycarbonate mold which then served as a template for casting 2% agarose wells. The agarose was separated into individual wells prior to cell seeding and culture. A cell suspension was then pipetted into agarose wells as shown schematically in **b** and **e** from the side and top, respectively (black dots represent individual cells). The cells were allowed to aggregate undisturbed for 48 h, which resulted in aggregation, contraction and tissue ring formation (**c** and **f**); black bands represent aggregated cells contracted around the post. Photographs of the side view (**d**) and the top view (**g**) of a 4-mm inside diameter tissue ring in an agarose well after 8 days in culture. Scale bars = 4 mm.
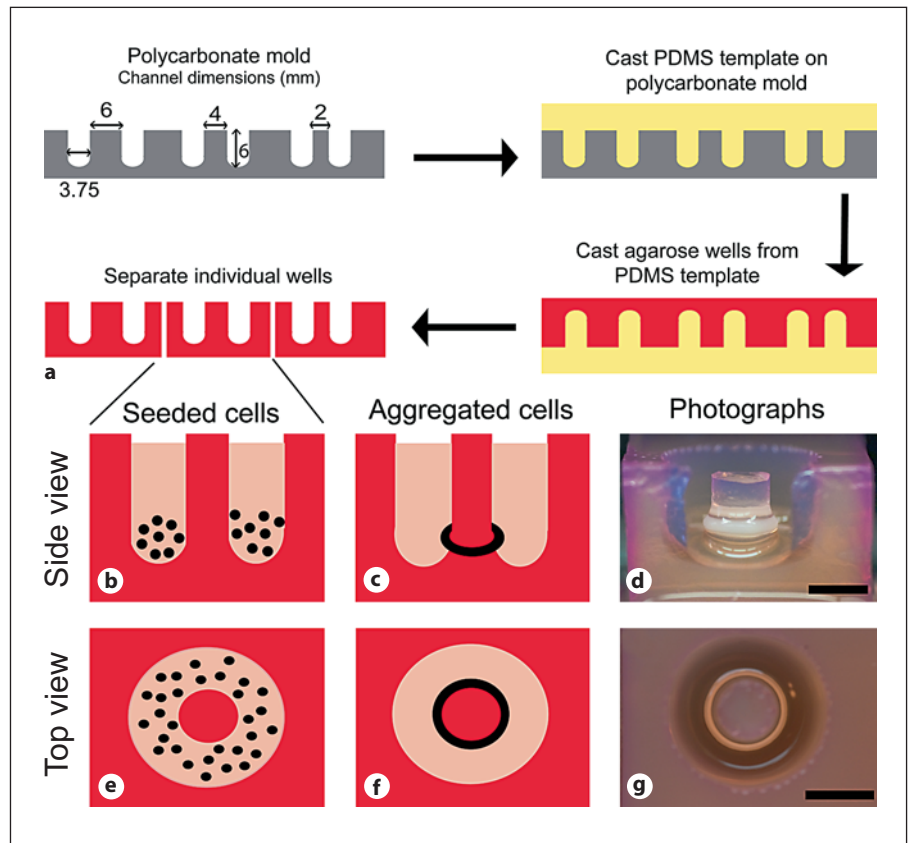
other to a 1 N (± 1 mN) load cell. Force (F) and displacement (Δl) were recorded continuously throughout the test at a frequency of 10 Hz. The measured thickness value described above was used to calculate the initial cross-sectional area, A, for each ring sample assuming a circular cross-section. A tare load of 5 mN was applied to the mounted ring and the gauge length (l_g) was recorded. The rings were then preconditioned for 8 cycles from the initial (tare) load to 50 kPa engineering stress (F/A) and then pulled to failure at a rate of 10 mm/min.

Engineering stress and grip-to-grip strain $(\Delta l/l_g)$ data were analyzed using MATLAB (The MathWorks Inc., Natick, Mass., USA) to obtain the ultimate tensile strength (UTS), failure strain, maximum tangent modulus (MTM, the maximum slope of the stress-strain curve) and toughness (area under the curve). The MTM is the maximum slope of the linear region of the curve and was used in these studies because it approximates the failure properties of the material to allow sample to sample comparisons, and compare our results to tissue constructs analyzed in other published studies cited in the Discussion section. The force at failure and the functional stiffness of the rings were also calculated as structural mechanical properties. The force at failure was recorded from the raw force data as a measure of the overall tissue strength. The product of the structural stiffness $(k,$ the maximum slope of the force-displacement curve; $F/\Delta l)$ and the gauge length, l_g, were calculated as a measure of the functional stiffness of the rings. This calculation was performed to normalize structural stiffness $(k)$ to the initial length of the sample in order to allow a fair comparison between samples with different inner diameters $(l_g \sim \frac{1}{2} \pi d_i)$. This metric, $k \cdot l_g$, can simply be obtained by multiplying the MTM of each sample by its initial cross-sectional area, that is, $(F/A)/(\Delta l/l_g) \cdot A = (F/\Delta l) \cdot l_g = k \cdot l_g$.

Histology

Tissue rings were fixed in 10% neutral buffered formalin and embedded in paraffin. Five-micrometer sections were cut and adhered to Superfrost Plus slides (VWR, West Chester, Pa., USA). The sections were stained with hematoxylin and eosin (H and E; reagents from Richard Allan Scientific, Kalamazoo, Mich., USA), Movat's pentachrome (reagents from Sigma, St. Louis, Mo., USA), Alcian Blue (American MasterTech Scientific Inc., Lodi, Calif., USA) and Fast Green/Picrosirius Red (reagents from Sigma; 0.1% each of Fast Green FCF and Direct Red 80 in picric acid), and images were acquired on an upright microscope (Leica DMLB2) equipped with a digital camera (Leica DFC 480). Polarized light images of samples stained with Picrosirius Red alone were acquired with an inverted microscope (Olympus IX81) with a digital camera (Olympus Q-Color 5). A linear polarizer was placed between the light source and the specimen, while the analyzer was installed in the light path between the specimen and the camera. The analyzer was rotated until maximum light diminishment was obtained prior to image acquisition from tissue samples. Under polarized light, small collagen I and III fibers appear green, whereas larger collagen I fibers appear yellow [Whittaker et al., 1994].
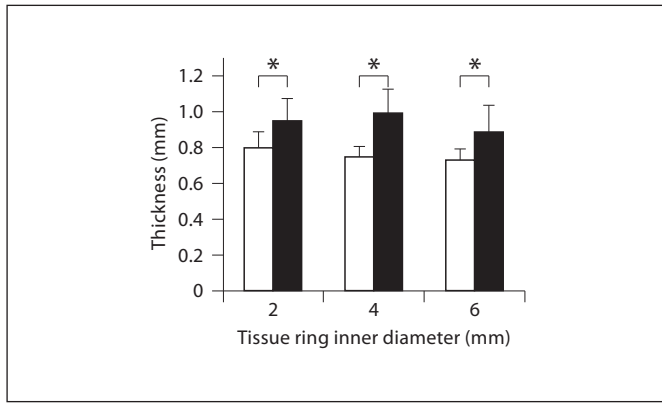
Fig. 2. Tissue ring thickness increased with culture time. Three thickness measurements were obtained for each ring sample (values are expressed as means ± SEM, * p < 0.05; n = 5–11 per group) cultured for 8 (white bars) or 14 days (black bars).
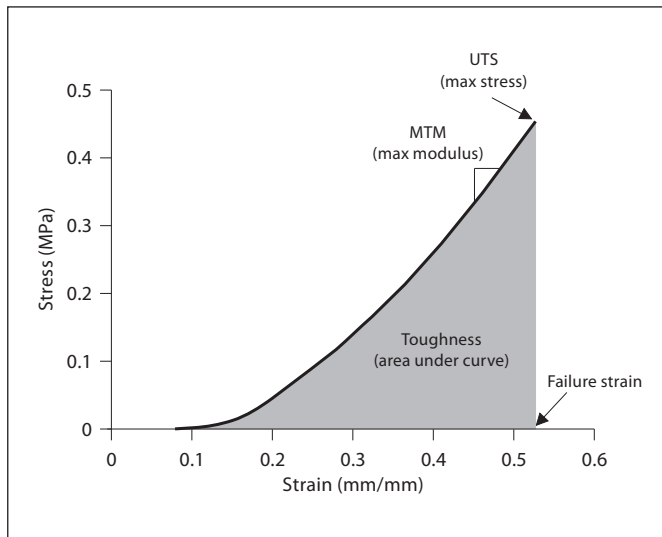
Fig. 3. Representative stress-strain data. A sample stress-strain curve obtained from a 4-mm tissue ring cultured for 8 days is shown with definitions of UTS, MTM, failure strain and toughness.

To visualize nuclei, deparaffinized, rehydrated histological sections were stained with Hoechst 33342 dye (10 μg/ml; Invitrogen, Eugene, Oreg., USA) for 3 min, rinsed with PBS and coverslipped with aqueous mounting medium (Prolong Gold; Invitrogen).

Tissue Ring Fusion for Cell-Derived Tube Fabrication

Cell-derived rings were created with 2-mm inner diameters and 500,000 cells per ring using the process described above. The rings were cultured for 7 days in agarose molds and then trans-

ferred onto 1.9-mm OD silicone tubes (SMI, Saginaw, Mich., USA). The rings were pushed into tight contact, the silicone was clamped into custom polycarbonate holders, and the rings were cultured horizontally for an additional 7 days. After a total of 14 days in culture (7 days as individual rings in agarose wells, 7 days grouped on silicone tubes), the aggregated tube-shaped samples were removed from the mandrels, fixed and processed for histology.

Statistics

Samples from 4 different batches of rings (2 for each time point) were analyzed to obtain sample sizes of 5–11 tissue rings per group for mechanical testing (8-day groups included 6, 8 and 5 tissue ring samples of 2, 4 or 6 mm inner diameter, respectively; 14 day groups included 6, 9 and 11 samples per 2-, 4- or 6-mm tissue ring group). The data are reported as means ± SEM for the tissue ring thickness values (3 measurements were obtained per ring sample) and as means ± SD for mechanical properties. A two-way ANOVA was used to analyze the effects of culture duration and ring inner diameter on tissue ring thickness and mechanical properties. SigmaPlot software (version 11.0, Systat Software Inc., Chicago, Ill., USA) was used to perform the ANOVA with Holm-Sidak post hoc analysis to identify significant differences (p < 0.05) between parameter values.

Results

Cells Aggregated and Formed Tissue Rings after Seeding into Agarose Wells

Representative photographs of tissue rings derived from aggregated SMCs are shown in figure 1. Within 48 h after seeding into agarose wells (the earliest time point examined), SMCs spontaneously aggregated to form rings that contracted around the center posts of nonadhesive, round-bottomed agarose wells. This aggregation was consistently observed for all rings generated, regardless of inner (post) diameter.

Tissue Ring Thickness Increased with Culture Time

Tissue ring thickness increased significantly with culture duration for rings of all sizes, from an average of 0.76 mm at 8 days to 0.94 mm at 14 days (19, 33 and 22% increase between 8 and 14 days for 2-, 4- and 6-mm rings, respectively; fig. 2). At each time point examined, there were no statistically significant differences in thickness between rings of different inner diameters (fig. 2).

Tissue Rings Were Mechanically Robust after only 8 Days of Culture

Stress-strain plots were generated from each of the tissue rings tested and used to calculate mechanical properties of tissue rings (a representative plot is shown in fig. 3). Eight days after cell seeding, larger tissue rings exhibited
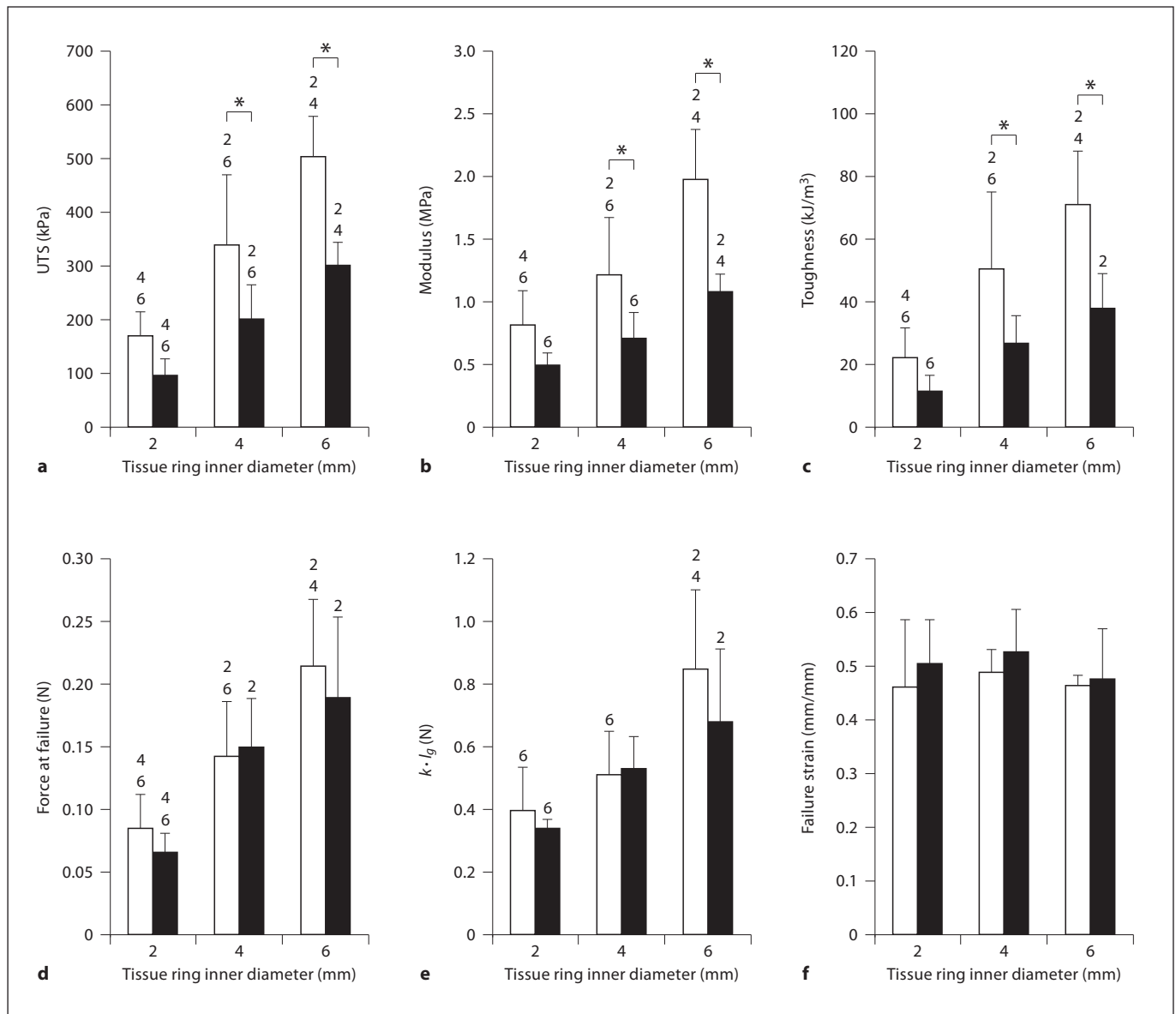
Fig. 4. Mechanical properties of cell-derived vascular tissue rings. Uniaxial tensile test results as a function of tissue ring inner diameter: **a** ultimate tensile strength (UTS), **b** modulus (maximum tangent modulus; MTM), **c** toughness, **d** force at failure, **e** $k \cdot l_g$ (functional stiffness), and **f** failure strain. All values are reported as mean ± SD; n = 5–11 per group. The asterisks indicate statistical differences between sample groups cultured for 8 (white bars) or 14 days (black bars) (p < 0.05). Numbers above the bars refer to the inner diameters of the sample groups cultured for the same time for which values are statistically different (p < 0.05).

greater UTS values than smaller rings (169 ± 45, 339 ± 131 and 503 ± 76 kPa for 2-, 4- and 6-mm rings, respectively; p < 0.05 for all comparisons, fig. 4a). Compared to 8 days of culture, the UTS was lower after 14 days [97 ± 30, 201 ± 63 and 302 ± 42 kPa, a decrease of 43% (not significant), 41% (p < 0.05) and 40% (p < 0.05) for 2-, 4- and 6-mm rings, respectively; fig. 4a). Tissue ring stiff-

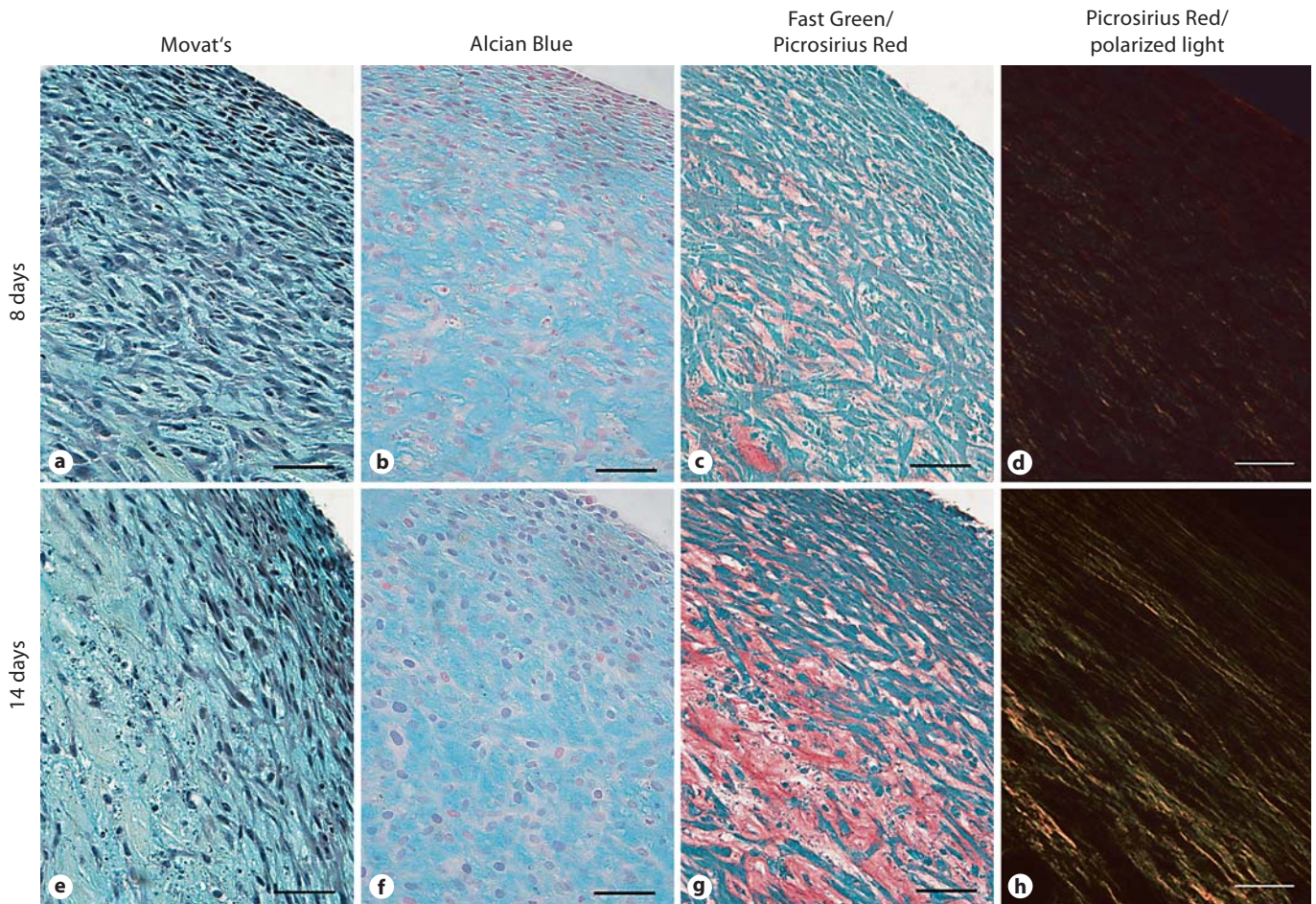ness (MTM) was similarly greatest in the largest rings after 8 days in culture (0.81 ± 0.28, 1.21 ± 0.46 and 1.98 ± 0.4 MPa, respectively, for 2-, 4- and 6-mm rings; fig. 4b). Similar to the UTS, the MTM values increased with post size by 33 and 59% for 4- and 6-mm rings compared to the 2-mm rings (p < 0.05 for all comparisons between ring diameters; fig. 4b). Further, the MTM de-
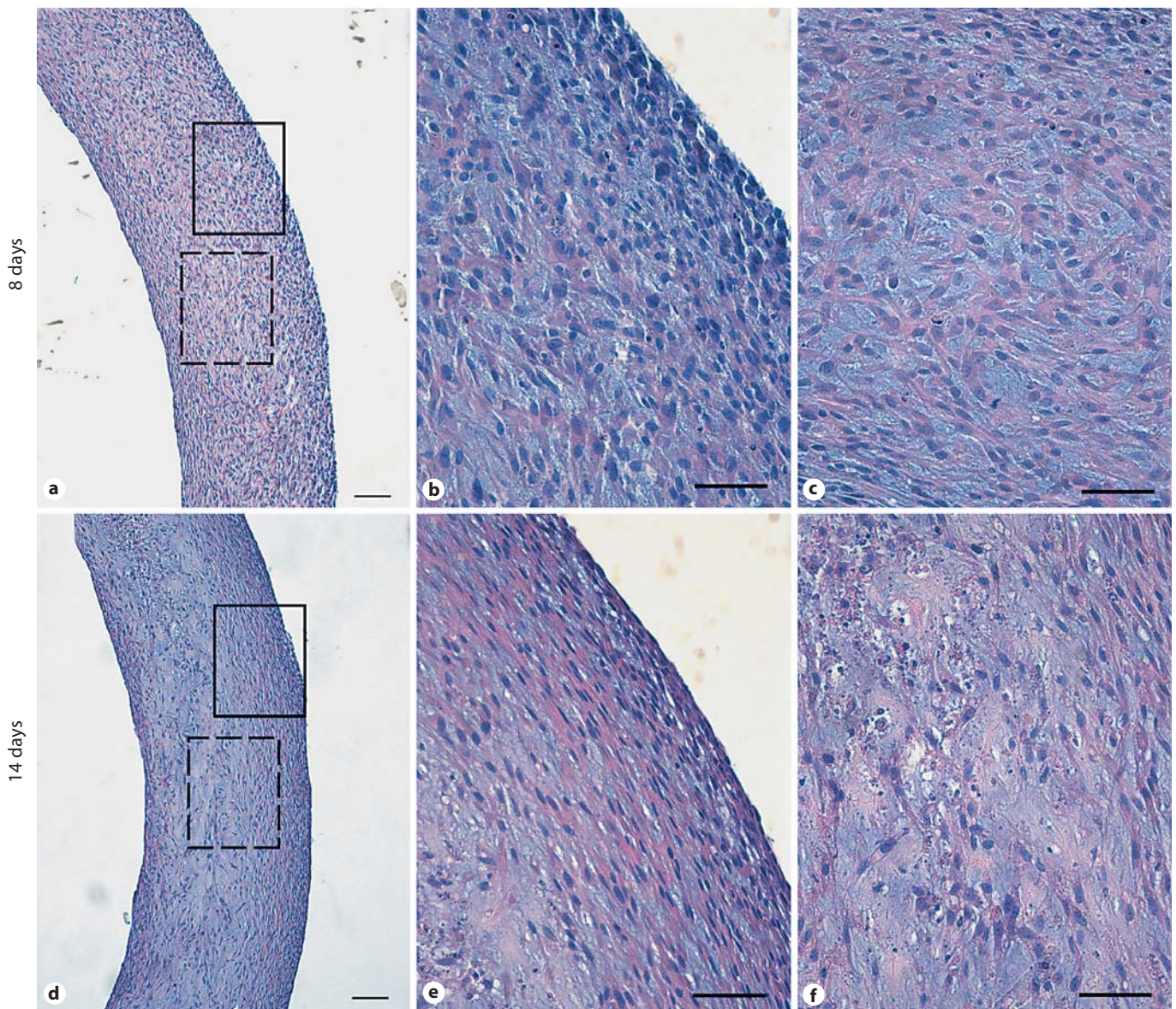
Fig. 5. Tissue ring morphology. Representative photomicrographs of 4-mm inner diameter tissue rings cultured for 8 (**a–c**) and 14 days (**d–f**). Low magnification views of the rings stained with H and E (**a**, **d**; scale bars = 100 μm) show the overall morphology of the rings. The boxes indicate the regions of interest magnified in **b**, **e** (solid boxes) and **c**, **f** (dashed boxes). Scale bars = 50 μm (**b**, **c**, **e**, **f**).

creased as a function of time in culture to 0.50 ± 0.09, 0.71 ± 0.20 and 1.08 ± 0.14 MPa for 2-, 4- and 6-mm rings at 14 days [a decrease of 39% (not significant), 41% (p < 0.05) and 45% (p < 0.05) for 2-, 4- and 6-mm rings, respectively; fig. 4b]. The toughness, or the ability of the tissue to absorb energy before rupture, decreased with culture time and increased with ring diameter in similar proportion to the changes in UTS (fig. 4c).

The structural properties also varied as a function of ring size. More force was required for failure of large rings (6 mm) than small rings (2 mm) at both time points (fig. 4d), and statistically significant increases in the functional stiffness metric $(k \cdot l_g)$ are observed with increasing ring size (fig. 4e). However, despite the observed changes in intrinsic properties (UTS and MTM) with culture duration, the structural properties are not sig-

Gwyther/Hu/Christakis/Skorinko/Shaw/
Billiar/Rolle

	Movat's	Alcian Blue	Fast Green/ Picrosirius Red	Picrosirius Red/ polarized light

Fig. 6. Histochemical assessment of tissue ring ECM composition. Movat's pentachrome (**a**, **e**) and Alcian Blue (**b**, **f**) staining indicated an abundance of sulfated glycosaminoglycans (blue) at 8 and 14 days of culture. Fast Green/Picrosirius Red staining (**c**, **g**) demonstrated the presence of collagen (red) at 8 and 14 days. Picrosirius Red staining alone observed under polarized light highlights yellow bands of collagen fibers (**d**, **h**). Scale bars = 50 μm.

nificantly different at 8 and 14 days. Further, the failure strain averaged 0.46 mm/mm for all samples with no statistical differences between sample groups of different size or culture duration (fig. 4f). Combined, these results indicated that the rings became thicker at 14 days but their structural properties did not change significantly between 8 and 14 days in culture.

Structure and Cellular Morphology of Tissue Rings
Representative micrographs of untested 4-mm rings are shown in figure 5. In tissue rings cultured for 8 or 14 days, cell density appeared highest along the edges of the rings (in direct contact with cell culture medium; fig. 5b, e), whereas the number of cells per area appeared to de-

crease at the centers of the rings (fig. 5c, f). In many regions along the circumference of the tissue rings, cells along both the inner and outer edges of the rings contained circumferentially aligned cells (fig. 5b, e), whereas cells at centers of the tissue rings did not appear aligned (fig. 5c, f). Additionally, the cells at the center of the thickest rings (cultured for 14 days) contained fragmented nuclei, which may indicate tissue necrosis (14-day samples; fig. 5f).

To more closely examine the composition of the tissue rings, histochemical stains were utilized to assess the composition of the tissue ring ECM (fig. 6). Movat's pentachrome and Alcian Blue staining showed that the predominant ECM components in the tissue rings after 8 or 14 days in culture are glycosaminoglycans (indicated by
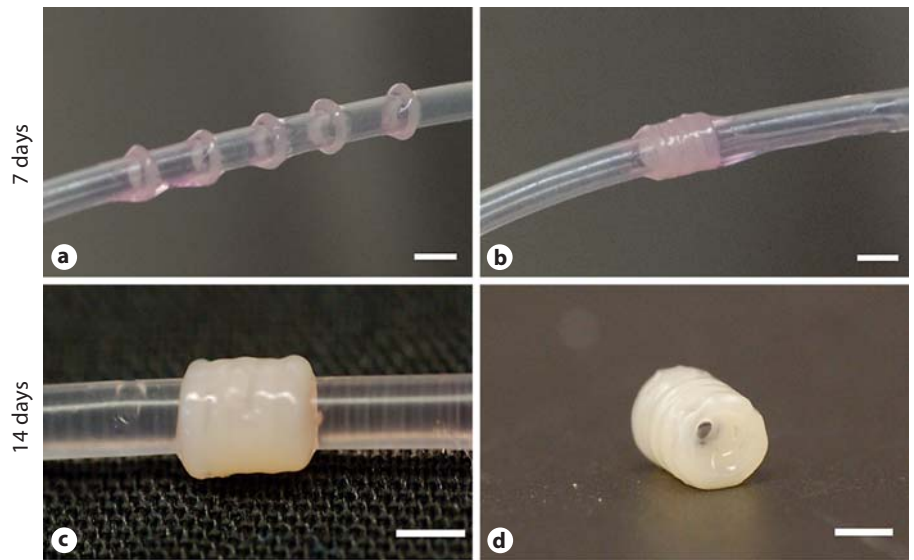
Fig. 7. Tissue ring fusion to form a tube. Tissue rings were cultured for 7 days before transfer onto a 1.9-mm outer diameter silicone mandrel (**a**) where they were placed in close contact (**b**). The tubes were then cultured for an additional 7 days (for a total of 14 days; **c**) before removal of the silicone mandrel to harvest the tissue tube (**d**). Scale bars = 2 mm.

the blue stain; fig. 6a, b, e, f). Collagen deposition was also detected and appeared to increase in quantity with culture time (red stain; fig. 6c, g). Examination of samples stained with Picrosirius Red by polarized light microscopy revealed that collagen quantity, circumferential alignment and fiber size (fig. 6d, h) increased with culture duration.
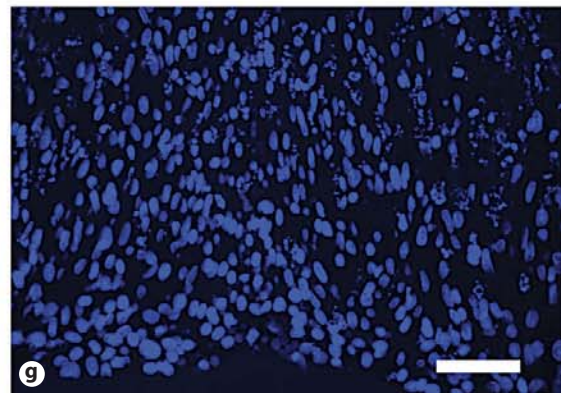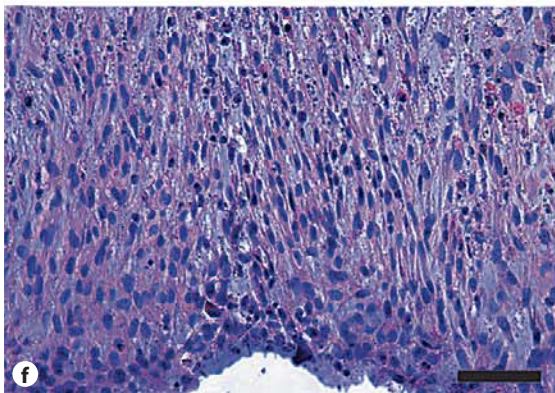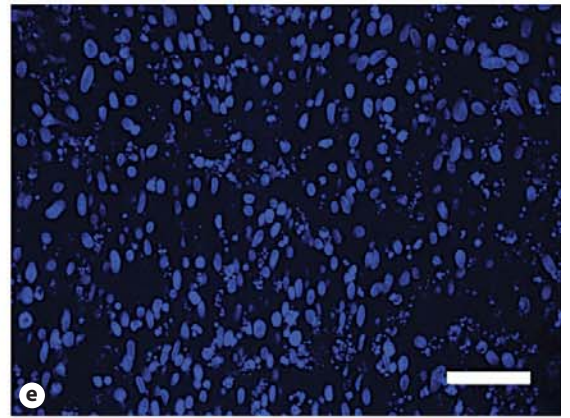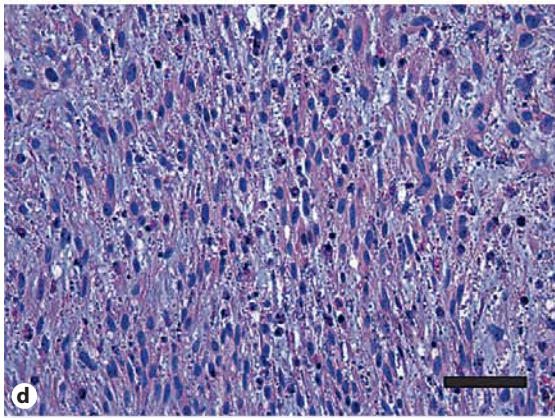
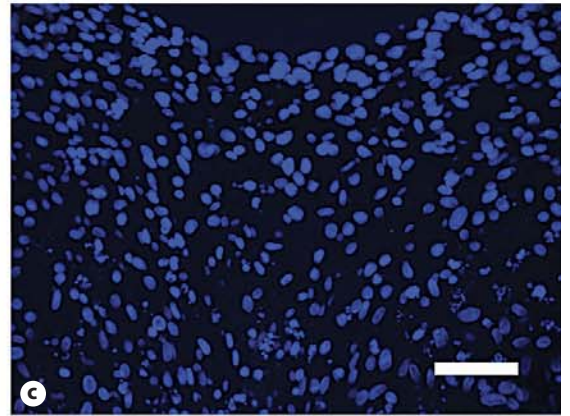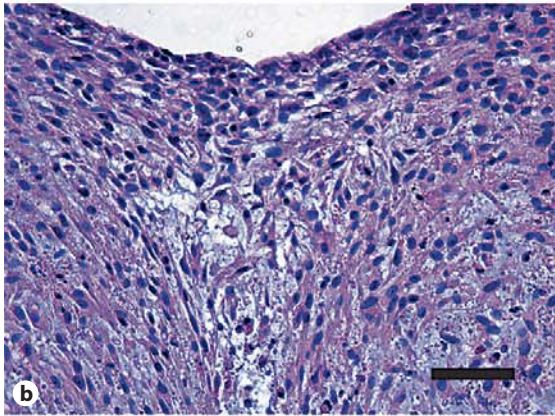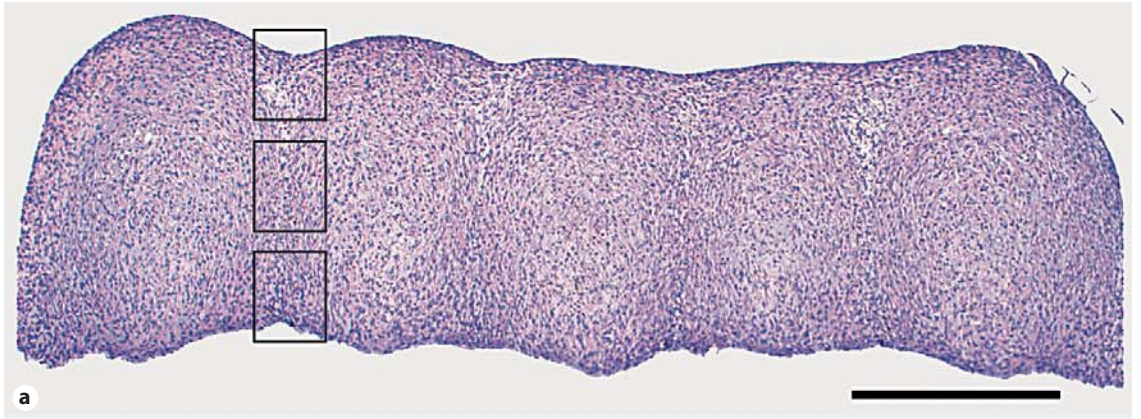*Translation of Rings to Tubes*

To assess the feasibility of using tissue rings as building blocks to create tissue tubes, 2-mm rings cultured for 7 days were removed from agarose wells, transferred to silicone tube mandrels (fig. 7a) and cultured in close contact (fig. 7b). Similar to 8- and 14-day rings tested in mechanical studies, 7-day rings were easy to handle and transfer. Individual rings become less distinct after 7 days in culture (fig. 7c), at which time cohesive tube constructs were successfully harvested from the silicone mandrels (fig. 7d). Tissue tubes remained intact during subsequent handling and processing for histological analysis. The original ring margins were still clearly visible by histology after 7 days of ring fusion (fig. 8a) with evidence of tissue reorganization and closure of 'gaps' between rings. Upon closer examination of the fusion junctions, the cells along the outer edge of the tube appear to form a healthy, contiguous cell layer (fig. 8b, c), whereas there are some fragmented nuclei at the centers of the tissue and along the central region of the fusion junction (fig. 8d, e). The nuclei on the inner edge (adjacent to the silicone mandrel; fig. 8f, g) also appear to form a contiguous layer that spans adjacent rings.

Discussion

We have developed and validated a method for fabricating ring-shaped tissue constructs entirely from aggregated SMCs that are strong enough to withstand handling and mechanical testing within 8 days of cell seeding. To our knowledge, this is the first study to report biomechanical evaluation of tissue constructs generated in a one-step process from aggregated cells and cell-derived ECM in static culture in this time frame. Our results demonstrate that facilitated cell aggregation can be used to create strong three-dimensional tissue constructs within the diameter range of clinically useful vascular grafts (2–6 mm). Although the focus of the current study was to characterize the strength and structure of ring-shaped constructs as a function of ring size and culture duration, we believe that this system will be useful for screening the effects of cell source and culture conditions on material properties of cell-derived tissues. Finally, we have provid-

Fig. 8. Tissue tube morphology. Representative photomicrographs of tissue tubes cultured for a total of 14 days (7 days as rings, 7 days on silicone mandrels). The tube appears completely fused, although ring margins are visible by H and E staining (**a**; scale bar = 0.5 mm). Higher magnification views of the junction between the first two rings are highlighted in three parts corresponding to the boxes in **a**; the outer junction (**b**, **c**), the middle junction (**d**, **e**), and the inner junction closest to the silicone tube (**f**, **g**) stained with H and E (**b**, **d**, **f**) and Hoechst nuclear dye (**c**, **e**, **g**). Scale bars = 50 μm (**b–g**).

ed evidence that these ring constructs can be used as building blocks to generate cell-derived tissue tubes, suggesting that information gained from functional ring studies may be directly translated to the design and construction of tubular structures such as vascular grafts.

Overall, cell-derived tissue rings were stronger than ring segments from engineered vascular tissue equivalents cultured for similar time periods. For example, the average UTS (100–500 kPa) far exceeded that reported for engineered tissues made with SMCs cultured statically within collagen (16 kPa at 8 days) [Seliktar et al., 2000] and collagen/fibrin mixtures (28 kPa at 7 days) [Rowe and Stegemann, 2006]. Without growth factor supplementation, the strength of our rings at 8 days approached that reported for SMC-populated fibrin gels cultured for 3 weeks with TGF-β1 and insulin (476 kPa) [Grassl et al., 2003]. The MTM (0.5–2 MPa) of the cell-derived tissue rings also compared favorably to other engineered tissue rings (0.07–5.35 MPa) [Seliktar et al., 2000; Gildner et al., 2004] and tissue ring toughness values (12–71 kJ/m^3) were also high relative to what has been observed for collagen gel-based model vessels (0.5 kJ/m^3) [Gildner et al., 2004]. However, all of these values are low compared to native arteries (for example, porcine carotid artery UTS approx. 6.6 MPa) [Dahl et al., 2007]. In future studies, optimization of culture conditions to increase ECM synthesis and tissue strength may be performed, such as treatment with soluble factors (for example, sodium ascorbate [Ahlfors and Billiar, 2007], TGF-β1 [Long and Tranquillo, 2003] and insulin [Long and Tranquillo, 2003]) or mechanical conditioning [Niklason et al., 1999; Isenberg and Tranquillo, 2003] to further strengthen cell-derived tissue rings.

Previous studies in which the strength and composition of planar cell-derived tissues were compared to constructs comprised of an equal number of cells seeded within fibrin or collagen gels demonstrated that cell-derived constructs exhibit greater tensile strength and ECM synthesis [Ahlfors and Billiar, 2007]. Similarly, robust synthesis of ECM, comprised primarily of glycosaminoglycans and collagen, may be the basis for the observed strength and stiffness of the cell-derived tissue rings. Quantitative biochemical analysis of ECM composition, organization and cross-linking will be performed in future studies to evaluate the molecular basis of tissue ring structure and material properties.

Ring size had a significant effect on tissue mechanical properties, with lower force at failure, UTS and MTM recorded for the smallest (2-mm) rings at all time points. Ring wall thickness was consistent across samples of different dimensions (cultured for the same duration; fig. 2),

therefore the length-to-cross-sectional-area ratio of the constructs at the initial gauge length differed as a function of ring inside diameter. We attempted to account for the effects of ring inside diameter by defining and reporting the functional stiffness (data shown in fig. 4e). As stated in the Methods section, this calculation was performed to normalize samples with different inner diameters ($l_g \sim \frac{1}{2}\pi d_i$). As a result of the high thickness-to-inside diameter ratio in smaller (2-mm) compared to larger (6-mm) rings, there may be greater bending stiffness associated with the smaller rings, therefore a greater load would be applied to the smaller rings to straighten them prior to pre-cycling. Consequently, the smaller rings may be subjected to higher stresses prior to the pull-to-failure test, which could result in lower recorded UTS and force at failure values in the 2-mm rings. However, regardless of the lower strength and modulus compared to larger rings, the 2-mm rings in this study were mechanically robust compared to those reported in other studies of engineered vascular tissue, as detailed above, and tissue ring fusion studies demonstrated that 2-mm rings cultured for 7 days were strong enough to withstand transfer and manipulation on silicone tubes. Histologically, the tissue rings were indistinguishable on the basis of size at a given time point (data not shown), and thickness and failure strain values were not statistically different.

Tissue ring wall thicknesses were greater (up to 0.94 mm after 14 days in culture) than those reported for other cell-derived tissue constructs. This may be partially explained by the high density of cell seeding used to form rings and greater proliferation rate of the rat cell line used in this study compared to primary human cells. By comparison, cell-derived tissue sheets generated from human dermal fibroblasts seeded at 10,000 cells/cm^2 and cultured for 6 weeks were 43 μm thick (more than 20-fold thinner), which increased by 5 μm per week thereafter (up to 15 weeks [L'Heureux et al., 2006]). Thicker constructs (125–395 μm) were created from human dermal fibroblasts within 3 weeks by seeding at a higher density (2 million cells seeded in a 4.5-cm^2 well) and culturing in chemically defined medium [Ahlfors and Billiar, 2007]. In our tissues, high thicknesses may have contributed to necrosis observed at the tissue centers. This necrosis may have contributed to a reduction in structural integrity due to a loss of cells, which may partially explain the observed decrease in UTS despite an increase in ring thickness between days 8 and 14. The polarized light microscopy data suggested that collagen synthesis and remodeling increased in the tissue rings between days 8 and 14, although this did not coincide with an increase in tissue

strength or stiffness. Interestingly, preliminary studies suggest that culturing tissue rings in culture medium supplemented with sodium ascorbate and amino caproic acid, conditions that have been shown to increase collagen synthesis and cross-linking, also improved tissue ring strength and stiffness (data not shown). It may be possible to optimize culture conditions (by decreasing or eliminating serum, and adding growth factors or mechanical stimulation, as described above) to make tissue rings stronger without increasing thickness.

Given the large number of cells needed to generate 4 batches of tissue rings in 3 different sizes to establish the basic parameters (for example, initial cell seeding number per well, culture duration and mechanical testing protocol) for creating and analyzing cell-derived tissue rings, we chose to use the WKY 3M-22 rat SMC line for the experiments reported in this study. However, we recently applied the same techniques to successfully assemble primary human coronary artery SMCs into cell-derived tissue rings, which were then cultured for 14 days. Despite their slower doubling time, in preliminary experiments the human SMC rings exhibited greater mechanical strength than the rat SMCs reported here (data not shown), thereby demonstrating that this cell aggregation system can be applied to create tissue rings from primary cells. Ongoing studies are focused on histological and biochemical analysis of the human SMC tissue constructs.

An important difference between the tissue ring constructs and vascular ring segments from native arteries is the lack of an endothelium or adventitia. Like many in vitro reports of TEBV construction, our study focused on a single cell type, SMCs, to mimic the vascular media. Recent studies have shown that cell sheet-based vascular grafts comprised of both SMCs and fibroblasts exhibit greater ECM synthesis and higher burst pressures compared to constructs made from SMCs alone [Gauvin et al., 2010]. Furthermore, microtissue aggregation studies have shown that endothelial cells can co-aggregate with fibroblasts to form spheroids [Napolitano et al., 2007a, b; Kelm et al., 2010]. It may therefore be possible to add fibroblasts and endothelial cells to SMCs to increase strength and more closely mimic blood vessel structure and function in cell-derived tissue rings.

Upon successful fabrication and handling of cell-based ring constructs, it became evident that cell-derived tissue rings could be used as building blocks to form tissue tubes. Here, we report proof of concept that tissue rings cultured in close proximity fuse to form a cohesive tissue tube within 14 days (7 days for ring fabrication and 7 days for fusion). Culturing the tubes for an extended period may result in further fusion and elimination of ring boundaries. A recent study by Livoti and Morgan [2010] showed that toroid microtissues (600 μm inner diameter) self-assembled from H35 hepatocytes cultured for 48 h could be stacked and cultured, with fusion of adjacent toroids within 72 h. The ease with which 2-mm SMC rings could be handled after 7 days in our study suggests that it may be possible to harvest our rings even earlier to accelerate the process of graft fabrication. Finally, histological evaluation demonstrated that individual rings had fused to form a contiguous tissue mass within 7 days. However, burst pressure analysis will be a critical benchmark to determine the feasibility of transplanting vascular grafts created with this method.

In conclusion, we have shown that tissue constructs that are suitable for manipulation and functional testing can be created from aggregated SMCs within a few days. Although these rings are not as strong as ring segments of native blood vessels or TEBV generated from cultured cell sheets for 2–3 months, their strength compares favorably to other engineered tissue constructs reported to date. Given the short time frame and simplicity of this system (which relies on commercially available materials and methods), it may enable systematic assessment of a variety of parameters on tissue structure and function (for example, cell source, culture medium composition and dynamic culture regimens). The ring-shaped geometry of these constructs is useful for mechanical testing, and based on the ease with which they could be mounted onto wire grips, may also be used in a myograph system to measure tissue responses to pharmacologic agents. This system has potential as a new three-dimensional in vitro model of vascular tissue function, and a versatile tool to advance development of cell-derived vascular grafts.

References

Ahlfors, J.E., K.L. Billiar (2007) Biomechanical and biochemical characteristics of a human fibroblast-produced and remodeled matrix. Biomaterials *28:* 2183–2191.

Dahl, S.L., C. Rhim, Y.C. Song, L.E. Niklason (2007) Mechanical properties and compositions of tissue engineered and native arteries. Ann Biomed Eng *35:* 348–355.

Gauvin, R., T. Ahsan, D. Larouche, P. Lévesque, J. Dubé, F. Auger, R. Nerem, L. Germain (2010) A novel single-step self-assembly approach for the fabrication of tissue-engineered vascular constructs. Tissue Eng Part A *16:* 1737–1747.

Gildner, C.D., A.L. Lerner, D.C. Hocking (2004) Fibronectin matrix polymerization increases tensile strength of model tissue. Am J Physiol Heart Circ Physiol *287:* H46–H53.

Grassl, E.D., T.R. Oegema, R.T. Tranquillo (2003) A fibrin-based arterial media equivalent. J Biomed Mater Res A *66:* 550–561.

Hashi, C.K., Y. Zhu, G.Y. Yang, W.L. Young, B.S. Hsiao, K. Wang, B. Chu, S. Li (2007) Antithrombogenic property of bone marrow mesenchymal stem cells in nanofibrous vascular grafts. Proc Natl Acad Sci USA *104:* 11915–11920.

Isenberg, B.C., R.T. Tranquillo (2003) Long-term cyclic distention enhances the mechanical properties of collagen-based media-equivalents. Ann Biomed Eng *31:* 937–949.

Kelm, J., V. Lorber, J. Snedeker, D. Schmidt, A. Broggini-Tenzer, M. Weisstanner, B. Odermatt, A. Mol, G. Zünd, S. Hoerstrup (2010) A novel concept for scaffold-free vessel tissue engineering: self-assembly of microtissue building blocks. J Biotechnol *148:* 46–55.

Konig, G., T. McAllister, N. Dusserre, S. Garrido, C. Iyican, A. Marini, A. Fiorillo, H. Avila, W. Wystrychowski, K. Zagalski, M. Maruszewski, A. Jones, L. Cierpka, L. de la Fuente, N. L'Heureux (2009) Mechanical properties of completely autologous human tissue engineered blood vessels compared to human saphenous vein and mammary artery. Biomaterials *30:* 1542–1550.

L'Heureux, N., N. Dusserre, G. Konig, B. Victor, P. Keire, T.N. Wight, N.A. Chronos, A.E. Kyles, C.R. Gregory, G. Hoyt, R.C. Robbins, T.N. McAllister (2006) Human tissue-engineered blood vessels for adult arterial revascularization. Nat Med *12:* 361–365.

L'Heureux, N., S. Paquet, R. Labbe, L. Germain, F.A. Auger (1998) A completely biological tissue-engineered human blood vessel. FASEB J *12:* 47–56.

Lemire, J., C. Covin, S. White, C. Giachelli, S. Schwartz (1994) Characterization of cloned aortic smooth muscle cells from young rats. Am J Pathol *144:* 1068–1081.

Lemire, J., S. Potter-Perigo, K. Hall, T. Wight, S. Schwartz (1996) Distinct rat aortic smooth muscle cells differ in versican/PG-M expression. Arterioscler Thromb Vasc Biol *16:* 821–829.

Livoti, C., J. Morgan (2010) Self-assembly and tissue fusion of toroid-shaped minimal building units. Tissue Eng Part A *16:* 2051–2061.

Long, J.L., R.T. Tranquillo (2003) Elastic fiber production in cardiovascular tissue-equivalents. Matrix Biol *22:* 339–350.

McAllister, T., M. Maruszewski, S. Garrido, W. Wystrychowski, N. Dusserre, A. Marini, K. Zagalski, A. Fiorillo, H. Avila, X. Manglano, J. Antonelli, A. Kocher, M. Zembala, L. Cierpka, L. de la Fuente, N. L'Heureux (2009) Effectiveness of haemodialysis access with an autologous tissue-engineered vascular graft: a multicentre cohort study. Lancet *373:* 1440–1446.

Mironov, V., R. Visconti, V. Kasyanov, G. Forgacs, C. Drake, R. Markwald (2009) Organ printing: tissue spheroids as building blocks. Biomaterials *30:* 2164–2174.

Napolitano, A.P., P. Chai, D.M. Dean, J.R. Morgan (2007a) Dynamics of the self-assembly of complex cellular aggregates on micromolded nonadhesive hydrogels. Tissue Eng *13:* 2087–2094.

Napolitano, A.P., D.M. Dean, A.J. Man, J. Youssef, D.N. Ho, A.P. Rago, M.P. Lech, J.R. Morgan (2007b) Scaffold-free three-dimensional cell culture utilizing micromolded nonadhesive hydrogels. Biotechniques *43:* 494, 496–500.

Nieponice, A., L. Soletti, J. Guan, B.M. Deasy, J. Huard, W.R. Wagner, D.A. Vorp (2008) Development of a tissue-engineered vascular graft combining a biodegradable scaffold, muscle-derived stem cells and a rotational vacuum seeding technique. Biomaterials *29:* 825–833.

Niklason, L.E., J. Gao, W.M. Abbott, K.K. Hirschi, S. Houser, R. Marini, R. Langer (1999) Functional arteries grown in vitro. Science *284:* 489–493.

Norotte, C., F. Marga, L. Niklason, G. Forgacs (2009) Scaffold-free vascular tissue engineering using bioprinting. Biomaterials *30:* 5910–5917.

Opitz, F., K. Schenke-Layland, T.U. Cohnert, B. Starcher, K.J. Halbhuber, D.P. Martin, U.A. Stock (2004) Tissue engineering of aortic tissue: dire consequence of suboptimal elastic fiber synthesis in vivo. Cardiovasc Res *63:* 719–730.

Rowe, S.L., J.P. Stegemann (2006) Interpenetrating collagen-fibrin composite matrices with varying protein contents and ratios. Biomacromolecules *7:* 2942–2948.

Seliktar, D., R.A. Black, R.P. Vito, R.M. Nerem (2000) Dynamic mechanical conditioning of collagen-gel blood vessel constructs induces remodeling in vitro. Ann Biomed Eng *28:* 351–362.

Shinoka, T., D. Shum-Tim, P. Ma, R. Tanel, N. Isogai, R. Langer, J. Vacanti, J.J. Mayer (1998) Creation of viable pulmonary artery autografts through tissue engineering. J Thorac Cardiovasc Surg *115:* 536–545; discussion 545–536.

Stegemann, J.P., S.N. Kaszuba, S.L. Rowe (2007) Review: advances in vascular tissue engineering using protein-based biomaterials. Tissue Eng *13:* 2601–2613.

Swartz, D.D., J.A. Russell, S.T. Andreadis (2005) Engineering of fibrin-based functional and implantable small-diameter blood vessels. Am J Physiol Heart Circ Physiol *288:* H1451–H1460.

Weinberg, C.B., E. Bell (1986) A blood vessel model constructed from collagen and cultured vascular cells. Science *231:* 397–400.

Whittaker, P., R.A. Kloner, D.R. Boughner, J.G. Pickering (1994) Quantitative assessment of myocardial collagen with picrosirius red staining and circularly polarized light. J Basic Research in Cardiology *89:* 397–410.

Zavan, B., V. Vindigni, S. Lepidi, I. Iacopetti, G. Avruscio, G. Abatangelo, R. Cortivo (2008) Neoarteries grown in vivo using a tissue-engineered hyaluronan-based scaffold. FASEB J *22:* 2853–2861.